The Interaction between H_2O and Preadsorbed O on the Stepped Pt(533) Surface

Maria J. T. C. van der Niet,*,† Otto T. Berg,†,‡ Ludo B. F. Juurlink,† and Marc T. M. Koper†

Leiden Institute of Chemistry, Leiden University, Einsteinweg 55, P.O. Box 9502, 2300 RA Leiden, The Netherlands, and Department of Chemistry, California State University, Fresno, 2555 East San Ramon MS SB/70, Fresno, California 93740, United States

Received: July 11, 2010; Revised Manuscript Received: September 21, 2010

We have investigated coadsorption of H_2O and O_{ad} on the stepped Pt(533) surface using temperature-programmed desorption in combination with isotope exchange. Water desorption from both bare and oxygen precovered Pt(533) gives rise to three easily identifiable peaks in the TPD spectrum between 140−210 K. Only in coadsorption experiments does a desorption feature at ∼270 K appear, which we ascribe to recombinative desorption of OH_{ad} on step sites. If the surface is saturated with O_{ad}, we also observe a broadening of the desorption peak at 188 K, indicative of OH formation on terrace sites. Oddly, the magnitude of the isotope exchange hardly varies with O_{ad} precoverage. Detailed analysis of the results suggest a strong bias for $OH_{terrace}$ formation over OH_{step} formation. This is likely related to the extent to which OH_{ad} can be incorporated into a larger hydrogen bonded network. In spite of the observation that OH_{step} is more strongly bound than $OH_{terrace}$, the overall exchange on the Pt(533) surface is much lower than on Pt(111).

Introduction

The interaction between water and platinum surfaces has been studied extensively because of its importance in electrochemistry, fuel cell catalysis, heterogeneous catalysis, and corrosion chemistry. Three extensive reviews have appeared that summarize the large body of knowledge on water−surface interactions that has been obtained using a variety of surfaces, coadsorbates, and employed techniques.[1−3] The interaction between H_2O, O_2, and platinum is especially interesting with regard to fuel cell catalysis, where OH adsorbed at platinum steps sites is considered to be a possible oxygen donor in oxidation reactions.[4,5] Another often studied process is the water formation reaction (WFR), where H_2 and O_2 react to form water via an OH intermediate. This reaction is also relevant for fuel cell catalysis and often studied as a prototype surface science reaction because of its relative simplicity.[6−11]

Most studies investigating the platinum−water interaction have used the (111) surface as a model for the catalytically active surface. Although this is the least complex system, ultra high vacuum (UHV) studies already show significant complexity in adsorption and desorption phenomena.[12−14] However, a real catalytic surface contains low coordination or defect sites in addition to (111) terraces. These defect sites are often thought to be more active for catalytic reactions involving bond breaking and making.[15] Although some experiments have focused on the influence of steps and defects that are naturally present on a Pt(111) crystal,[16,17] more insight should result from studies employing a better defined model, such as a regularly stepped surface.[10,18]

The general consensus is that on Pt(111) water adsorbs molecularly at all coverages and temperatures (<180 K). Even prolonged exposure to X-rays does not cause dissociation in the water layer.[19] Classically, water adsorbed on metal surfaces is thought to form an icelike bilayer of hexagonal rings.[1−3] Low-energy electron diffraction (LEED)[20] and helium diffraction[21] images show a $(\sqrt{37} \times \sqrt{37})R25.3°$ structure for H_2O islands formed at sub-monolayer (ML) coverage, which is compressed into a $(\sqrt{39} \times \sqrt{39})R16.1°$ structure for the full bilayer. A combined scanning tunneling microscopy (STM) and density functional theory (DFT) study finds these $\sqrt{37}$ and $\sqrt{39}$ phases to also contain pentagon and heptagon structures.[22] An extensive high-resolution electron energy loss spectroscopy (HREELS) study by Jacobi et al. shows distinct differences in the vibrational spectra for water monomer, bilayer, and multilayer structures.[23] Water dosed on Pt(111) at temperatures well below 135 K leads to the formation of amorphous solid water (ASW).[24] Temperature programmed desorption (TPD) studies of ASW show two peaks. One peak at 171 K is associated with monolayer desorption. This peak exhibits the characteristics of zero-order desorption kinetics[25] and has been attributed to the coexistence of a condensed phase and a 2-dimensional water−gas at sub-monolayer coverages.[24] A second peak, associated with desorption from multilayers, starts at 154 K and increases in temperature with coverage.[26]

Only a few studies have been performed on the interaction between H_2O and stepped platinum surfaces.[10,16−18,27,28] STM studies on an imperfect Pt(111) crystal show that water adsorbs preferentially on step sites, forming molecular chains.[16] TPD shows a stabilization of the water monolayer by the presence of step sites.[10,18,27−29] A two-peak structure is observed for a monolayer of H_2O desorbing from the stepped Pt(533) surface (Pt[4(111) × (100)]). At coverages below 0.13 ML_{H_2O} a single peak is observed, which is reported to shift with coverage from 184 to 188 K.[18,27] This peak is associated with desorption from step sites. At higher coverage (above ∼0.33 ML_{H_2O}) a shoulder appears at 171 K, which is associated with desorption from terrace sites. The peak associated with desorption from the water multilayer appears at ∼150 K.[18,27] Water binds stronger to (110) than to (100) steps.[28]

Oxygen adsorbs in three different states on Pt(111): physisorbed O_2 molecules are stable below 45 K,[30] chemisorbed O_2 molecules below 100−200 K,[31] and atomic oxygen below

* To whom correspondence should be addressed: E-mail: jvanderniet@chem.leidenuniv.nl.
† Leiden University.
‡ California State University.

10.1021/jp106412e
Published on Web 10/20/2010

575−900 K.[31] Subsurface oxygen is reported between 1000 and 1200 K if the sample is annealed between these temperatures at high oxygen pressures.[31] Oxygen dissociation is activated, and atomic oxygen formation occurs via a precursor state of molecularly adsorbed oxygen. This precursor mechanism causes the sticking coefficient to decrease with surface temperature.[32,33] The maximum O_{ad} coverage that can be reached via background dosing is 0.25 ML_{Pt}. LEED[31,34−38] and STM[39] pictures show a (2 × 2) pattern. Oxygen atoms bind preferentially in the fcc hollow sites.[40,41]

On stepped surfaces a similar (2 × 2) LEED-pattern is observed for O_{ad} as on Pt(111).[42,43] However, Fiorin et al. state that no ordered structure of O_{ad} atoms is formed on Pt(211) and Pt(411).[44] Dissociation takes place at 200 K[45] on the (111) terrace but occurs predominantly on step sites[33,46−48] between 150 and 230 K.[44,45,49] Oxygen atoms adsorb preferentially on step sites.[39,48] A combined STM and DFT study[39] shows that for (100) steps a 2-fold edge bridging site is favored, whereas for (110) steps the fcc hollow site behind the step edge is favored. O_{ad} atoms bind stronger on (100) steps than on (110) steps.[28,44] TPD spectra on Pt(533),[28,33,45,46,50] other surfaces with (100) steps,[49,51,52] and surfaces with (111) steps[28,34,42,43,53] all show a three-peak structure in the molecular oxygen regime and a two peak structure in the atomic oxygen regime. Equilibration between step and terrace sites happens only above 400 K.[46] Oxygen atoms do not diffuse onto the lower lying terrace.[48]

The coadsorption of H_2O and O_2 on Pt(111) is known to produce OH_{ad} for $150 \leq T \leq 185$ K.[19,54,55] When $^{18}O_2$ and $H_2^{16}O$ are coadsorbed at sub-monolayer coverages and subsequently annealed, the ratio ^{18}O:^{16}O desorbing in H_2O is 1:2, independent of the initial $H_2^{16}O$ coverage. Surface OH groups do not readily exchange H with unreacted O_{ad}.[56] From this stoichiometry initially

$$2H_2O_{ad} + O_{ad} \rightarrow 3OH_{ad} + H_{ad} \quad (1)$$

was deduced as the reaction equation.[56,57] However, recent DFT calculations found that this reaction does not go to completion, and the H_{ad} is actually incorporated in a hydrogen bonded network of H_2O_{ad} and OH_{ad}[58,59] via

$$2H_2O_{ad} + O_{ad} \rightarrow H_2O_{ad} + 2OH_{ad} \quad (2)$$

All O_{ad} participates in the OH formation.[19] This produces a $(\sqrt{3} \times \sqrt{3})R30°$ LEED pattern with a weak (3 × 3) superstructure.[55,57,60] H_2O is needed to stabilize the formed OH species.[19,61] Different structures can be produced by different O_{ad}: H_2O ratios. The maximum number of H_2O molecules that can participate in the reaction with one O adatom is four. However, the stoichiometry in eq 2 produces the most stable structure.[60] The hydrogen bonded network consists of hexagonal rings of coplanar O atoms bonded near atop sites with different O−O separations. All H groups participate in the hydrogen bonded network, and OH is always bonded to the platinum substrate via the oxygen atom. All hydrogen bonds lie parallel to the surface.[55,62] One third of the shared protons is delocalized between two O atoms, making them neither clearly covalently bound nor hydrogen bonded to the oxygen atoms.[63] The OH/H_2O overlayer does not have H-bonds left to bind to a second layer, which makes the surface hydrophobic.[64] When H_2O is removed, two OH react again to form immediately desorbing H_2O (g) and O_{ad}. Water desorption from the O-covered surface does not follow simple kinetics and happens through multiple channels: direct desorption, via OH recombination, as well as through proton transfer mediated transportation of water to the edges of an OH/H_2O cluster.[65] Desorption happens primarily at low coordination and defect sites in the OH/H_2O overlayer. HREELS studies on Pt(111) show three separate δ (OH_{ad}) peaks at 127, 113, and 102 meV, attributed to structurally different OH groups. The two lower energy peaks are due to OH groups which are hydrogen bond donors but not acceptors.[57] The formed OH_{ad} is also the intermediate in the WFR. In the presence of the gas phase H_2 it reacts readily to form H_2O.[9]

No studies have been performed regarding the interaction between O_{ad} and H_2O on stepped platinum surfaces. This system is particularly interesting, since step-bonded hydroxyl is considered the oxygen donor in many electrocatalytic oxidation reactions. The peak observed between 0.6 and 0.9 V vs the reversible hydrogen electrode (RHE) in the blank cyclic voltammetry of Pt(111) is generally considered to be due to the adsorption of OH from dissociated H_2O on terrace sites.[66] At higher potentials OH_{ad} is converted into O_{ad}. Because of its "buried" nature in aqueous solution, applying vibrational spectroscopy to identify OH is problematic. Therefore, evidence regarding the nature of the voltammetric feature is by exclusion of other possible adsorbates. On stepped platinum surfaces the electrochemical oxidation of CO starts already at 0.4 V. This indicates that OH has to be present at steps sites at 0.4 V.[67] However, no direct evidence has been found of the presence of OH_{ad} at these potentials. More insight into the nature of OH groups on stepped platinum surfaces is thus required. Therefore, an attempt to isolate OH at step sites on platinum would be very interesting.

We have studied the interaction between O_{ad} and H_2O on the stepped Pt(533) surface, which consists of 4 atom wide (111) terraces and a (100) step. The sample is studied under UHV conditions using TPD and LEED in combination with isotope exchange. We have discussed the main differences between this surface and the Pt(553) surface in an earlier publication.[68] Here we give a more elaborate account of the results for the Pt(533) surface.

Experimental Section

Experiments were performed in a UHV apparatus, described in detail elsewhere,[69,70] with a base pressure of 2×10^{-10} mbar during experiments. The Pt(533) crystal was cleaned by repeated cycles of Ar^+ bombardment (Messer, 5.0, 3−4 μA, 20 min), annealing between 850 and 1000 K in an oxygen atmosphere (2×10^{-8} mbar, Messer, 5.0) and annealing at 1200 K. LEED (and Auger) spectra were taken with a microchannel back-display LEED/Auger (Vacuum Microengingeering, optics: BLD800IR, miniature electron gun: G10, controller: LPS300-D). LEED images taken after these cleaning procedures give a spot row spacing to spot splitting ratio of ∼3.24, which corresponds well to literature values.[71] Water from a Millipore Milli-Q gradient A10 system (18.2 MΩ cm resistance) was deaerated in a glass container by multiple freeze−pump−thaw cycles and then kept at a total pressure of 1.2 bar He (Linde gas, 5.0). The container was connected to a home-built glass capillary array doser located in the infrared cell of the UHV apparatus. Water was dosed directly on the surface at a rate of ~ 0.007 ML_{H_2O} s^{-1} by measuring the pressure rise due to the codosed helium. Both $^{16}O_2$ and $^{18}O_2$ (Cambridge Isotope Laboratories, 97% isotope purity, ≥99.9% chemical purity) were dosed by background dosing (usually 0.4 L). The amount of adsorbed oxygen was then controlled by annealing the sample

at a fixed temperature for 5 min in order to boil off unwanted oxygen. In the case of a fully saturated surface a flash to 250 K proved sufficient to remove any molecular O_2. Care was taken not to heat the sample too fast in order to allow enough molecularly adsorbed O_2 to dissociate. All reported pressures are uncorrected for ion gauge sensitivity.

During TPD experiments the sample was placed in a collinear geometry with a differentially pumped quadrupole mass spectrometer (QMS, Balzers QMS 422). The heating rate was always 1 K s^{-1}. During heating $m/e = 18$ ($H_2^{16}O$), 20 ($H_2^{18}O$), 32 ($^{16}O_2$), 34 ($^{16}O^{18}O$), and 36 ($^{18}O_2$) were monitored. Gee and Hayden[33] observed an angle dependence for the sticking probability of O_2 on Pt(533). This could indicate that the angular distribution of O_2 desorbing from Pt(533) is not uniform as well. Therefore, the use of the differentially pumped QMS might influence the relative intensities of oxygen desorbing from step and terrace sites. We tested this by comparing the TPD spectra from the differentially pumped QMS with spectra obtained with the QMS (Balzers, QMS 420) inside the main vacuum. No difference was observed in the spectra, indicating that the housing of the differentially pumped QMS is located close enough to the sample for angle dependent effects not to be of influence. Preliminary measurements were taken during which also $m/e = 2(H_2)$ and 38 ($H_2^{18}O_2$) were monitored. These measurements showed no desorption of these compounds. All H_2O and O_{ad} coverages are calculated from the integrated TPD peak areas. Analogous to Gee and Hayden[33] we assume the maximum O_{ad} coverage to be 0.25 ML_{Pt}. Our exact definition of a water monolayer (ML_{H_2O}) is given in the Results and Discussion.

Since H_2O sticks to the stainless steel walls of the differentially pumped QMS chamber, the high vacuum time constant of H_2O leads to an almost stepwise increase in the baseline of our H_2O TPD spectra. A reasonable approximation for the baseline is given by

$$y = y_0 + \frac{1}{2}\Delta y\left(\tanh\left(\frac{T - T_0}{\Delta T}\right) + 1\right) \qquad (3)$$

where Δy is the total increase in the height of the baseline, T_0 is the center of the S curve, typically slightly before the peak maximum, and ΔT is an arbitrary parameter to smooth out the tanh. Note that the value of ΔT does not affect the total obtained integral, though it may affect the relative intensities of smaller peaks at lower temperatures. We have verified that this baseline correction procedure does not influence the leading edges of our TPD data when fixing ΔT for a given set of data.

Results and Discussion

O_2 Adsorption/Desorption. We have shown and discussed the TPD spectra of the single species (O_2 and H_2O) in a previous publication.[28] Here, we only summarize our main findings. Figure 1a shows the $^{16}O_2$ TPD spectrum with the maximum coverage we could obtain. The $^{16}O_2$ was dosed at $T_{crys} \approx 100$ K. The low-temperature peak at 664 K is associated to the recombinative desorption of O_{ad} on the (111) terraces.[33] The high-temperature peak at 775 K is associated to the recombinative desorption of O_{ad} from step sites.[33] The ratio $O_{ad,\,step}$: $O_{ad,\,ter}$ as determined by Gaussian fits is approximately 0.11: 0.14.[28]

Flashing to 250 K removes all molecularly adsorbed oxygen from the Pt(533) surface and ensures that all remaining oxygen is dissociated into atomic oxygen. When the fully oxygenated surface is annealed at 650 K oxygen adatoms from terrace sites

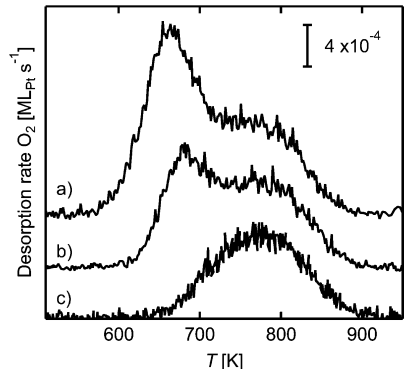

Figure 1. (a) TPD spectrum of O_2 desorbing from Pt(533) obtained by dosing 0.4 L O_2 (enough to maximally cover the surface with O_{ad}). (b) After annealing for 5 min at 610 K. (c) After annealing for 5 min at 640 K.

recombine into O_2 and desorb, leaving less O_{ad} on the surface for the subsequent TPD, resulting in the spectrum show in Figure 1c, where only the step sites remain covered with O_{ad}. Annealing at lower temperatures leaves intermediate amounts of O_{ad} on the surface (e.g., 610 K results in the spectrum shown in Figure 1b). Annealing between 650 and 735 K partially desorbs O_{ad} from step sites as well. If the surface is annealed at $T > 750$ K, no desorbing O_2 can be detected in the subsequent TPD spectrum. Hydrogen TPDs taken after annealing the oxygen covered surface to 860 K (to just boil off the oxygen) show no change in the amount of step and terrace sites compared to the freshly prepared surface, indicating that no significant O-induced surface reconstruction has occurred.

In the isotope exchange experiments $^{18}O_2$ was used instead of $^{16}O_2$. In this case 3% of the predosed O_{ad} on the surface is ^{16}O and 97% ^{18}O due to contamination from background gas. The isotope exchange data are uncorrected for this effect. When $^{18}O_2$ is present on step sites only and consecutively $^{16}O_2$ is dosed on the terrace sites, the O_2 TPD shows both species desorbing from both step and terrace sites. The ratio ^{16}O:^{18}O is identical for both peaks, indicating that oxygen adatoms on the step and terrace sites have fully equilibrated. Equilibration between step and terrace O has previously been found to occur above 400 K only.[46] Since H_2O is only present on the surface at temperatures below 320 K, we do not believe that this equilibration influences the exchange between preadsorbed O_{ad} and H_2O_{ad}. However, it is not possible to tell whether the desorption of an oxygen isotope from a step or terrace site specifically is due to reaction at that site with H_2O or due to the equilibration at higher temperatures. Therefore, we will only discuss the total oxygen signals and not the site specific contributions to the signal when discussing the oxygen exchange data.

H_2O Only. Figure 2c shows TPD spectra for $m/e = 18$ and 20 after dosing various amounts of $H_2^{16}O$ onto a bare Pt(533) surface. We have discussed these results previously.[27,28] Briefly, H_2O desorbs in three peaks, α_1, α_2, and α_3, with peak temperatures of ~188, ~171, and ~148 K, respectively. The peak at highest temperature, α_1, appears at the lowest H_2O coverages. At coverages <0.25 ML_{H_2O} the peak desorption temperature shows a slight increase from 184 to 188 K with increasing dose. For $\theta_{H_2O} < 0.25$ ML_{H_2O}, we observe no shift in desorption temperature until saturation of the α_1 peak. The second peak, α_2, is clearly observed prior to saturation of α_1. We interpret this observation as proof of limited mobility of H_2O molecules adsorbed onto this surface. The lowest temperature peak, α_3, is only observed when α_1 and α_2 have saturated. Following Grecea et al.,[18] we use the largest combined integral

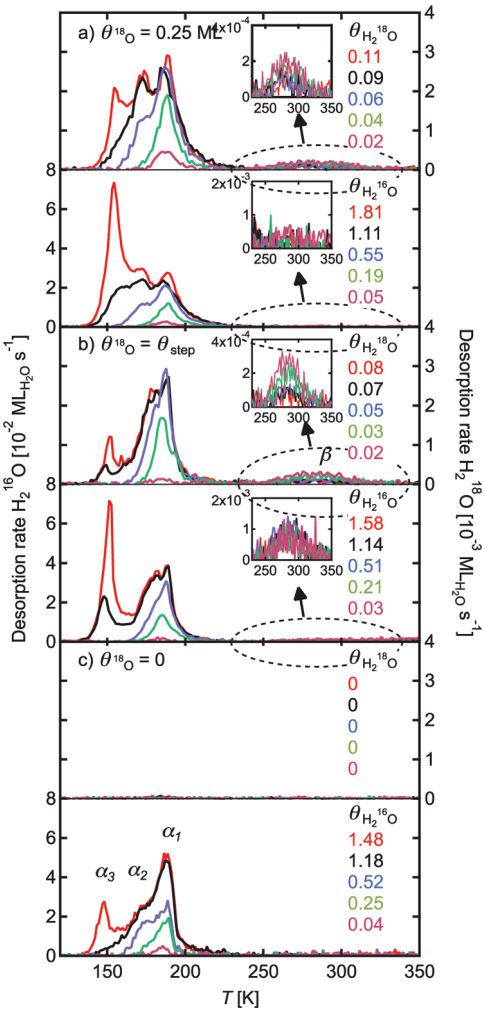

Figure 2. TPD spectra of $H_2^{16}O$ (left axis) and $H_2^{18}O$ (right axis) dosed on Pt(533) with (a) $\theta_{^{18}O} = 0.25$ ML_{Pt}, (b) $\theta_{^{18}O} = \theta_{step}$, and (c) $\theta_{^{18}O} = 0$.

for α_1 and α_2 as a reference for the amount of adsorbed H_2O and refer to this amount as $\theta_{H_2O} = 1$ ML_{H_2O}. The ratio α_1:α_2 as determined by Gaussian fits is roughly 5:4. This indicates that sites which bind water more strongly than the (111) plane are much more abundant than would be expected from geometrical arguments: sites adjacent to step sites are also influenced. Dosing larger quantities leads to the appearance of the α_3 peak, which is the result of multilayer desorption.[18] The spectra show a discrepancy in the absolute desorption temperatures compared to the ones reported by Grecea et al.,[18] which has been addressed in a previous publication.[27] When we inspect the $H_2^{18}O$ signal, we observe that adsorbing $H_2^{16}O$ on bare Pt(533) leads to no measurable desorption of $H_2^{18}O$.

Co-Adsorption of $^{18}O_{ad}$ and $H_2^{18}O$. $\theta_{^{18}O} \approx \theta_{step}$. Figure 2b shows TPD spectra for $m/e = 18$ and 20 after dosing various amounts of $H_2^{16}O$ onto a Pt(533) surface where all step sites have been precovered with ^{18}O. First we focus on the $H_2^{16}O$ spectra (lower part, plotted vs left axis). Similar to the bare surface, we observe a three peak structure. The peak temperatures are roughly the same as well. The α_1 desorption temperature slightly increases from 184 to 188 K between 0 and 0.25 ML_{H_2O}. The α_2 peak starts to appear at 182 K as a shoulder to α_1, before α_1 saturates, at $\theta_{H_2O} > 0.50$ ML_{H_2O}. The multilayer peak, α_3, appears at ~150 K for $\theta_{H_2O} > 0.90$ ML_{H_2O}, after saturation of α_1 and α_2. Thus, α_1 and α_3 have not shifted compared to the bare surface, whereas α_2 has shifted from 171 to 182 K. This indicates an extra stabilization of terrace water by the O adatoms on step sites. If we look closely at the peak shapes and integrals, we notice that these have changed compared to $\theta_{^{18}O} = 0$, i.e., the ratio α_1:α_2 is smaller in the $\theta_{^{18}O} \approx \theta_{step}$ case. The α_2 peak has broadened slightly at the low temperature side. This could either be explained by relatively more H_2O desorbing from terrace sites or a decrease in the difference in adsorption energy for step and terrace sites. We also observe that the water multilayer forms at lower water coverages than for the bare surface. This is probably due to competition between O adatoms and H_2O molecules for adsorption on step sites. This would lead to less H_2O on step sites and would thus explain the decrease in magnitude of α_1.

Next we turn to the $H_2^{18}O$ signal (upper part of Figure 2b, plotted vs right axis). Here, we first note that we have not unambiguously determined the integral for 1 ML_{H_2O} $H_2^{18}O$ desorbing from the surface, we have used the integral for 1 ML_{H_2O} $H_2^{16}O$ as our reference in calculating $\theta_{H_2^{18}O}$. We feel this is justified since the ionization efficiency in our QMS, the transmission through the quadrupole, and the amplification by the channeltron are not expected to vary significantly for these isotopes. Turning to the data, we observe that the α_1 and α_2 peaks behave similar to the $H_2^{16}O$ signal, though the α_2 peak appears to be slightly smaller than in the $H_2^{16}O$ signal. The main difference is that the signal is lower by a factor of 10. The α_3 peak is relatively much smaller. $H_2^{18}O$ desorption starts at 142 K, indicating that eq 2 occurs reversibly at (and quite possibly below) this temperature. The small amounts of $H_2^{18}O$ in α_3 show that the exchange between the first and second water layer is poor.

A new broad feature (β) is observed at ~270 K. The β peak is hardly discernible in the $H_2^{16}O$ signal in the figure. However, here we would like to point out the scale difference of a factor of 10 in the spectra. The feature has to be due to an attractive interaction between H_2O and the adsorbed O atoms on step sites. Possible species formed are $(H_2O)_x-O_y$, OH, or O + H. OH is known to be stable on Pt(111)[19,54,55,58,60] and is thus a likely candidate for the species formed at step sites.

OH has to be stable on a surface for the WFR to occur. It is an intermediate species in the reaction, but it has been shown on Pt(111) that its stability makes the WFR occur efficiently, since it catalyzes the reaction.[7,9,72,73] On Pt(111) all O_{ad} is completely removed by the WFR when the oxygenated surface is kept at 135 K (well below the desorption temperature of atomic oxygen (700 K)[43]) in a hydrogen atmosphere.[6] Therefore, we can test whether OH is stable on the Pt(533) surface by use of the WFR. We have held a Pt(533) surface with $\theta_O \approx \theta_{step}$ under a H_2 pressure of 2×10^{-7} mbar at 200 K. The surface temperature of 200 K was chosen to desorb all formed H_2O immediately. The subsequent oxygen TPD shows no desorbing oxygen. The $O_{ad,\,step}$ can only have been removed by the WFR if the formed OH_{ad} is stable. Therefore, we conclude that OH has to be stable at step sites. On Pt(111) the stable OH causes H_2O to desorb at higher temperatures, i.e., 200 K instead of 170 K for the bare surface.[60,74] On the stepped Pt(533) surface this effect is more dramatic, showing an increase of 80 K from 188 to 270 K. Therefore, a plausible albeit tentative explanation for the high temperature β peak is that it is due to reaction of OH_{step} to form H_2O. Spectroscopic techniques should provide more definitive insight in this matter.

The intensity of the β peak in the $H_2^{18}O$ signal is dependent on H_2O coverage, being larger for lower θ_{H_2O}. In the $H_2^{16}O$ signal this effect is not observed, but the absolute magnitude of the peak is five times larger, which probably masks this subtle effect.

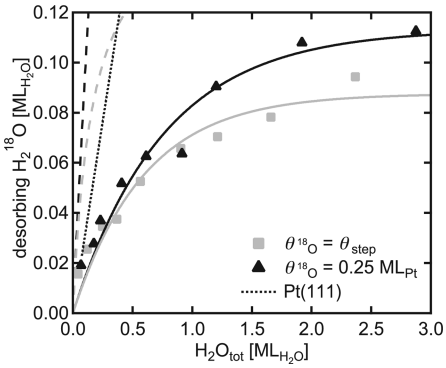

Figure 3. Isotopic partitioning vs the amount of adsorbed $H_2^{16}O$ for Pt(533) with $\theta_{^{18}O} = \theta_{step}$ (gray squares) and $\theta_{^{18}O} = 0.25$ ML_{Pt} (black triangles). The inset shows the absolute amount of desorbing $H_2^{18}O$. The lines fitted through the data are only a guide for the eye. The dashed lines show calculated traces for complete isotopic scrambling, whereas the dotted line shows the same data for desorption from a Pt(111) surface precovered with 0.25 ML_{Pt} O taken from ref 56.

The appearance of the α_3 peak in the $H_2^{18}O$ spectra indicates that eq 2 occurs reversibly at low temperatures. As the reversible eq 2 already occurs below 140 K, we expect that ^{18}O is leached by $H_2^{16}O$, leading to a decrease of the β peak in the $H_2^{18}O$ signal with increasing $H_2^{16}O$ coverage.

The gray data in Figure 3 show the absolute amount of desorbing $H_2^{18}O$ as a function of the total amount of desorbing H_2O for $\theta_{^{18}O} \approx \theta_{step}$. We compare this to the amount of $H_2^{18}O$ formed on Pt(111)[56] as well as to complete isotopic scrambling, assuming a similar Pt:H_2O ratio in 1 ML_{H_2O} as found on Pt(111),[1−3] i.e., 3:2. The amount of exchange taking place on the Pt(533) surface is far less than if complete isotopic scrambling were to occur. The amount of $H_2^{18}O$ formed increases with increasing $H_2^{16}O$ dose, whereas the relative amount of $H_2^{18}O$ drops with increasing H_2O coverage to 6% (not shown here). This is consistent with the fact that α_1 and α_2 do not increase in size in the $H_2^{18}O$ signal in Figure 2b when $\theta_{H_2O} > 0.90$ ML_{H_2O}. Since the coupling to the second layer was shown to be poor, the relative exchange as a function of θ_{H_2O} levels off. We will discuss these data further in the next subsection.

Figure 4a shows the isotopic partitioning of ^{16}O and ^{18}O in the TPD spectra of the recombinative desorption of O_{ad} from step sites. The dashed line shows the calculated partitioning if complete scrambling occurs. Since we have concluded from Figure 2b that isotope exchange between layers is poor, we have assumed no further exchange above $\theta_{H_2O} = 1$ ML_{H_2O} in the complete scrambling scenario. Complete scrambling is clearly not the case. At low $H_2^{16}O$ coverages most O_{ad} on the surface after water desorption is still ^{18}O. When the $H_2^{16}O$ coverage reaches 0.25 ML_{H_2O} 50% of the $^{18}O_{ad}$ has been exchanged with ^{16}O from $H_2^{16}O$. The exchange saturates at ∼75% of all O_{ad}. STM shows that at low H_2O coverages most molecules are located at step sites.[16] Therefore, below 0.25 ML_{H_2O} most water is likely located at the steps. Oxygen adatoms are not mobile on the surface below 400 K,[46] and all O_{ad} is also located at the step. At low coverages all extra adsorbed water is in direct contact with the oxygen adatoms adsorbed at the steps. At higher coverages additional water will be adsorbed at terrace sites and probably not interact with the oxygen atoms on step sites. Therefore, this additional water is not likely to contribute to the isotope exchange. An isotopic partitioning of more than 50% ^{16}O indicates that each oxygen adatom has interacted with more than one H_2O molecule, either by direct contact or by eq 2 occurring reversibly at low temperatures, moving ^{18}O in water to terrace sites or the multilayer, and allowing further exchange

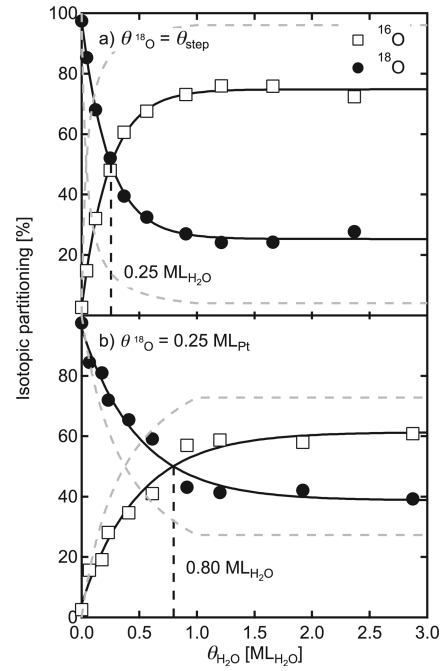

Figure 4. Isotopic partitioning in oxygen TPD spectra, taken from the m/e = 32, 34, and 36 signals, for varying amounts of $H_2^{16}O$ dosed on Pt(533) precovered with (a) $\theta_{^{18}O} = \theta_{step}$ or (b) $\theta_{^{18}O} = 0.25$ ML_{Pt}. The dashed gray lines show calculated traces for complete isotopic scrambling.

with $H_2^{16}O$ molecules at these sites. The presence of the α_2 and α_3 peaks in the $H_2^{18}O$ spectra makes it impossible to fully exclude the latter explanation. However, we have already argued that coupling to the multilayer is inefficient. The α_2 peak is present in the $H_2^{18}O$ spectra, but it is smaller compared to the $H_2^{16}O$ spectra. Therefore, we think most O is exchanged via a direct interaction between O_{ad} and H_2O. If this is the case, one O_{ad} atom on step sites interacts with up to three H_2O molecules. This is less than on Pt(111), where up to four H_2O molecules can interact with one O adatom.[60] This could be due to the broken symmetry of the surface, introduced by the presence of step sites. Since the O_{ad} is located at the top of the step and is slightly puckering out of the step edge,[39] it is conceivable that some of these H_2O molecules are located at the bottom of the step.

θ^{18}_O = 0.25 ML_{Pt}. Figure 2a shows TPD spectra for m/e = 18 and 20 after dosing various amounts of $H_2^{16}O$ onto a Pt(533) surface where both step and terrace sites have been precovered with ^{18}O. We still observe three peaks in the $H_2^{16}O$ signal (lower half, plotted vs left axis). The peak temperatures are identical to the ones on the bare surface: α_1 ∼188 K, α_2 ∼171 K, and α_3 ∼155 K. However, the α_1 peak has become somewhat broader at the high temperature side compared to both $\theta_{^{18}O} = 0$ and θ_{step}. It is located at a similar position as the feature caused by oxygen-induced OH formation on Pt(111), which varies between 195 and 205 K for different O_{ad} precoverages.[74] Therefore, it would be difficult to observe separate peaks for recombinative desorption of H_2O from OH on terrace sites and H_2O desorbing from step sites, but the sum of these peaks could be observed as a broadened α_1 peak. Thus the broadening of the α_1 peak suggests OH formation at terrace sites. The multilayer peak, α_3, is already present at coverages well below 0.9 ML_{H_2O}, which is a lower coverage than in the $\theta_{^{18}O} \approx \theta_{step}$ case, where we ascribed this to competition between O_{ad} and H_2O on step sites. We ascribe the further lowering of the combined $\alpha_1-\alpha_2$ integral to a similar competition of O_{ad} with H_2O for adsorption sites

both on steps and terraces. The $H_2^{18}O$ signal (upper half of Figure 2c, plotted vs right axis) behaves similar to the $\theta_{^{18}O} \approx \theta_{step}$ case: the α_1 and α_2 peaks are smaller versions of the ones in the $H_2^{16}O$ signal, whereas the α_3 feature is relatively small. We do not observe the slight decrease in the α_2 peak, as was the case on the $\theta_O \approx \theta_{step}$ surface. The appearance of $H_2^{18}O$ in the multilayer peak indicates that $^{18}O-^{16}O$ exchange has begun below ~155 K, but H_2O exchange between the first and second H_2O layers remains limited.

Also in this case we observe a small β peak at ~270 K, albeit slightly smaller compared to the θ_{step} case. In the $H_2^{16}O$ signal it may be lost in the noise. This indicates that the extra O adatoms on terrace sites disfavor OH formation at step sites. Possibly, H_2O molecules near the step edge are more inclined to interact with O_{ad} on terrace sites than with O_{ad} on step sites as we argued before for Pt(553).[68,75]

The black triangular data points in Figure 3 show the absolute amount of $H_2^{18}O$ desorbing as a function of the total amount of desorbing H_2O for $\theta_{^{18}O} = 0.25$ ML_{Pt}. The amounts formed are far less than in case of complete isotopic scrambling, or desorption from the Pt(111) surface. At H_2O coverages <0.25 ML_{H_2O}, the amount of $H_2^{18}O$ formed is independent of oxygen precoverage (the black and the gray traces are identical). The step sites were always fully covered with O_{ad} in both sets of experiments. At these low coverages water preferentially adsorbs at step sites, as has been shown previously for the bare surface by STM.[16] All adsorbed water is in contact with O_{ad} at low coverages. As the amount of H_2O increases the traces start to differ. For $\theta_{^{18}O} = 0.25$ ML_{Pt} the maximum amount formed is ~0.11 ML_{H_2O} or 5%. This is only 1.2 times the amount we measured for $\theta_{^{18}O} \approx \theta_{step}$. However, from the ratio $O_{ad,\,step}$:$O_{ad,\,ter}$ obtained from Figure 1a it is clear that there is over twice as much ^{18}O present on the surface. The increase in formed $H_2^{18}O$ upon also precovering terrace sites with ^{18}O is far less than would be expected based on this ratio. This could suggest that on the Pt(533) surface $O_{ad,\,terrace}$ is less active in the isotope exchange with H_2O than $O_{ad,\,step}$. For the Pt(553) surface, however, we have argued that at high O_{ad} precoverages not $O_{ad,\,terrace}$ is inactive in the oxygen exchange but $O_{ad,\,step}$. We based this on two observations. First, in TPD spectra with $\theta_O = \theta_{max}$ a peak is present at 193K, which is a similar position as the recombinative OH desorption peak on Pt(111).[60] Second, the peak associated with recombinative desorption of OH from step sites decreases in both size and desorption temperature compared to $\theta_O \approx \theta_{step}$.[68,75] Even though these effects are much more subtle on the Pt(533) surface, we do observe them; the α_1 peak has broadened if we compare the $\theta_O = 0.25$ ML_{Pt} to the θ_{step} spectra, which could very well be due to an overlap between the original α_1 peak and a peak due to recombinative OH desorption around 192 K. We also observe a decrease in the magnitude of the β peak compared to the θ_{step} case. On Pt(111) it has been shown that OH_{ad} has to be incorporated in a hydrogen bonded OH/H_2O network.[19,61] On Pt(533) this can be done more easily on terrace than on step sites, favoring $OH_{terrace}$ formation over OH_{step} formation, even though for a single OH (i.e., in the absence of water) step sites may be more favorable adsorption sites. This also explains why stepped surfaces are far less reactive for eq 2 than Pt(111).

Figure 4b shows the isotopic partitioning in O_2 for $\theta_{^{18}O} = 0.25$ ML_{Pt}. At the lowest H_2O coverages the isotopic partitioning is similar to when $\theta_{^{18}O} \approx \theta_{step}$. However, the isotopic partitioning of ^{16}O desorbing as O_2, i.e., O adatoms that have exchanged with the O atoms in $H_2^{16}O$, rises less steeply than was the case when only the step sites were precovered with ^{18}O. When $\theta_{H_2^{16}O}$ ≈ 0.80 ML_{H_2O} half of the $^{18}O_{ad}$ on the surface has been exchanged with ^{16}O. The isotopic partitioning levels off at ~61%, showing that on average only two H_2O molecules interact with one O adatom. This is less than when only the step sites were covered with O_{ad}, where it was three. The isotopic exchange saturates earlier for $\theta_{^{18}O} \approx \theta_{step}$ than for $\theta_O = 0.25$ ML_{Pt}. This shows that when terrace sites become occupied with oxygen adatoms, at higher water coverages, not all O_{ad} interacts with H_2O. Possibly, also for the fully oxygenated Pt(533) surface not all H_2O molecules are participating in the OH/H_2O network. This is in contrast with findings for Pt(111), where all adsorbed H_2O is part of the OH/H_2O network.[64] On stepped platinum surfaces, in the presence of water, terrace OH is favored over OH_{step}. On terraces it is possible to form hexagonal water rings, incorporating the OH_{ad} formed. In spite of more favorable energetics for forming a single OH on step sites, the possibility of being incorporated in a large network appears to favor the formation of OH on terrace sites for the system as a whole.

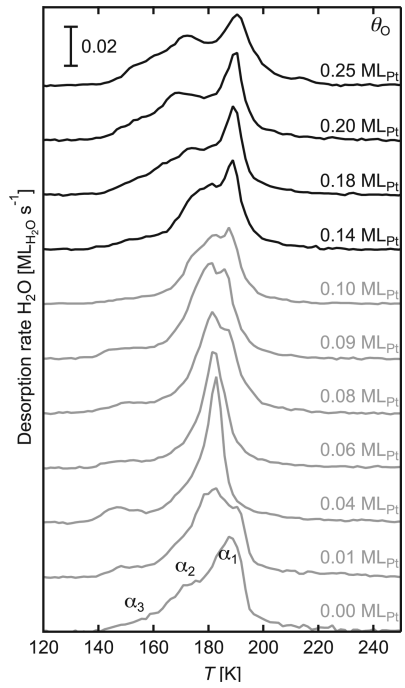

Figure 5. TPD spectra of ~1 ML_{H_2O} H_2O desorbing from Pt(533) with varying O_{ad} precoverages of the steps sites (gray) and the full step and part of the terrace sites (black).

The (111) terrace on our Pt(533) crystal is only just large enough to form one water hexagon. This is probably too little to form an entire stable OH/H_2O structure, causing the presence of step sites to form a break in this network, excluding some O (and H_2O) from participating in the oxygen exchange. The stability of the formed OH/H_2O structure is likely to vary with terrace width. A study on the amount of exchange on surfaces with different terrace widths could provide more insight.

Varying ^{18}O Precoverages. Figure 5 shows the TPD spectra for ~1 ML_{H_2O} H_2O adsorbed on the Pt(533) surface with varying O_{ad} precoverages. In the lower half (gray traces) of Figure 5 the amount of preadsorbed O on step sites has been varied. When no oxygen is adsorbed we observe the three peak structure ($\alpha_1-\alpha_3$) shown in Figure 2c. As step sites become covered with preadsorbed oxygen the α_1 peak initially decreases in size, whereas the α_2 peak increases in size. Some H_2O_{step} is converted into OH_{step} and desorbs in the β peak (not shown in Figure 5). This (partially) lifts the step induced stabilization of other H_2O molecules that now desorb in α_2. H_2O is pushed from the α_1

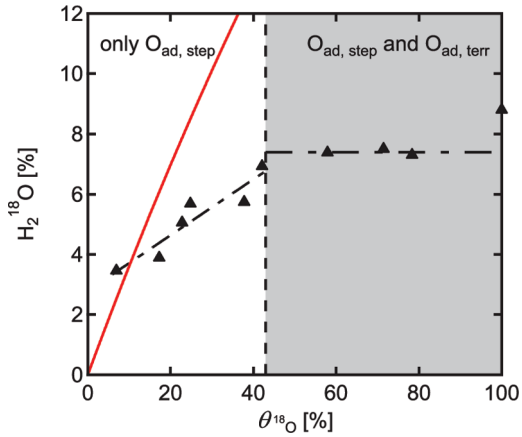

Figure 6. Isotopic partitioning of $H_2^{18}O$ vs the amount of preadsorbed $^{18}O_2$ when Pt(533) is covered with $ML_{H_2O} \sim 1$ $H_2^{16}O$. The dashed line marks the coverage from which the (111) terrace starts to become occupied with $^{18}O_{ad}$. The straight line shows the amount of exchange if complete isotopic scrambling were to occur.

into the α_2 peak, resulting in a two-peak structure (a single $\alpha_1 + \alpha_2$ peak, either due to two overlapping peaks or a new peak representing a new structure, and a separate α_3 peak) at $^1/_3\theta_{step} \lesssim \theta_O \lesssim {}^2/_3\theta_{step}$. At higher coverages the three peak structure emerges again. However, initially the α_2 peak is larger than the α_1 peak and very sharp. The α_1 peak becomes larger than α_2 again only when the step sites are almost fully covered with oxygen (>0.09 ML_{Pt}). The disappearance and reappearance of the α_1 peak with increasing O_{ad} precoverage corroborates the theory that at high θ_O this peak is actually due to a different processes than at low θ_O, i.e., at high θ_O it is due to recombinative desorption of OH from terrace sites.

The top half of Figure 5 shows the TPD spectra for the Pt(533) surface where the terrace sites are also precovered with varying amounts O_{ad}. A three peak structure is visible in all spectra. At coverages $\gtrsim {}^1/_2\theta_{terrace}$ the TPD features broaden toward the high temperature side, showing the onset of OH formation on the (111) terraces. Initially less H_2O desorbs in the α_2 peak. When the surface is fully oxygenated the α_1 peak also correponds to less H_2O. This illustrates the increasing competition of H_2O with O_{ad} for adsorption sites.

The percentage of $H_2^{18}O$ desorbing as a function of the surface $^{18}O_{ad}$ precoverage for ~ 1 ML_{H_2O} postdosed $H_2^{16}O$ is given in Figure 6. The straight line shows the calculated amount of exchange for complete isotopic scrambling. For O_{ad} coverages up to 43% of the surface only the step sites are covered with $^1O_{ad}$ (white area). The relative amount of $H_2^{16}O$ that has exchanged an oxygen atom with $^{18}O_{ad}$ increases linearly in this regime from ~3 to ~7%. The gray area in the graph shows the regime where the terrace sites become occupied with preadsorbed $^{18}O_{ad}$. In this regime the percentage of exchanged O stays roughly constant at 8%. With increasing oxygen precoverage, O adatoms have to compete with one another for interaction with H_2O molecules. This causes the amount of exchange in H_2O to be constant with increasing O_{ad}, whereas the percentage desorbing as O_2 decreases slightly (not shown here). Except for the lowest θ_O the amount of exchange is far less than if complete isotopic scrambling were to occur, suggesting again that O_{ad} in steps is much more stable (against OH_{ad} formation) in steps than it is on terraces.

Conclusion

We have shown that the coadsorption of H_2O and O_{ad} on the Pt(533) surface gives rise to a small new feature at ~270 K in the H_2O TPD spectra, tentatively ascribed to OH_{ad} on step sites. If the full surface is precovered with O_{ad} we also observe a broadening of the α_1 peak, which we ascribe to OH-formation on terrace sites. Varying the O_{ad}:H_2O ratio shows that different ratios give rise to various structures in the TPD spectra, indicating that there are different stable structures possible on the surface, similar to Pt(111).[60] We believe that hexagonal ring structures on terraces are favored whenever possible, at the expense of the formation of step-bonded OH that is energetically more favorable if only that species is taken into account. Isotope exchange data show that when only the step sites have been precovered with O_{ad} the O_{ad} interacts with up to three H_2O molecules. The exchange does not increase much when more ^{18}O is present on the surface. We attribute this to competition between OH formation on step and terrace sites. Terrace sites are favored, because there the formed OH can be incorporated in a larger hydrogen bonded structure. A discontinuity in this surface structure by the presence of the step causes the overall reactivity toward the formation of OH to be lower than on Pt(111).

Generally it is found that reactivity increases with the amount of defects.[15] The formation of OH on step sites is a counter-example to this common observation. This shows that experiments on Pt(111) surfaces are a poor model for the reactivity of catalytic particles, since they do not take into account these defect sites. The stability of the formed OH/H_2O structure is likely to vary with terrace width. A study on the amount of exchange on surfaces with different terrace widths could provide more insight into this issue.

Acknowledgment. We kindly thank prof. Aart W. Kleyn and FOM for use of equipment. This work was supported financially by The Netherlands Organization for Scientific Research.

References and Notes

(1) Thiel, P. A.; Madey, T. E. *Surf. Sci. Rep.* **1987**, *7*, 211–385.
(2) Henderson, M. A. *Surf. Sci. Rep.* **2002**, *46*, 1–308.
(3) Hodgson, A.; Haq, S. *Surf. Sci. Rep.* **2009**, *64*, 381–451.
(4) Lebedeva, N. P.; Rodes, A.; Feliu, J. M.; Koper, M. T. M.; van Santen, R. A. *J. Phys. Chem. B* **2002**, *106*, 9863–9872.
(5) García, G.; Koper, M. T. M. *Phys. Chem. Chem. Phys.* **2009**, *11*, 11437–11446.
(6) Ogle, K. M.; White, J. M. *Surf. Sci.* **1984**, *139*, 43–62.
(7) Mitchell, G. E.; Akhter, S.; White, J. M. *Surf. Sci.* **1986**, *166*, 283–300.
(8) Verheij, L. K.; Hugenschmidt, M. B. *Surf. Sci.* **1998**, *416*, 37–58.
(9) Völkening, S.; Bedürftig, K.; Jacobi, K.; Wintterlin, J.; Ertl, G. *Phys. Rev. Lett.* **1999**, *83*, 2672–2675.
(10) Skelton, D. C.; Tobin, R. G.; Fisher, G. B.; Lambert, D. K.; DiMaggio, C. L. *J. Phys. Chem. B* **2000**, *104*, 548–553.
(11) Nagasaka, M.; Kondoh, H.; Amemiya, K.; Nambu, A.; Nakai, I.; Shimada, T.; Ohta, T. *J. Chem. Phys.* **2003**, *119*, 9233–9241.
(12) Zimbitas, G.; Hodgson, A. *Chem. Phys. Lett.* **2006**, *417*, 1–5.
(13) Kimmel, G. A.; Petrik, N. G.; Dohnálek, Z.; Kay, B. D. *J. Chem. Phys.* **2006**, *125*, 044713.
(14) Zimbitas, G.; Haq, S.; Hodgson, A. *J. Chem. Phys.* **2005**, *123*, 174701.
(15) Vattuone, L.; Savio, L.; Rocca, M. *Surf. Sci. Rep.* **2008**, *63*, 101–168.
(16) Morgenstern, M.; Michely, T.; Comsa, G. *Phys. Rev. Lett.* **1996**, *77*, 703–706.
(17) Ogasawara, H.; Yoshinobu, J.; Kawai, M. *J. Chem. Phys.* **1999**, *111*, 7003–7009.
(18) Grecea, M. L.; Backus, E. H. G.; Riedmüller, B.; Eichler, A.; Kleyn, A. W.; Bonn, M. *J. Phys. Chem. B* **2004**, *108*, 12575–12582.
(19) Shavorskiy, A.; Gladys, M. J.; Held, G. *Phys. Chem. Chem. Phys.* **2008**, *10*, 6150–6159.
(20) Harnett, J.; Haq, S.; Hodgson, A. *Surf. Sci.* **2003**, *528*, 15–19.
(21) Glebov, A.; Graham, A. P.; Menzel, A.; Toennies, J. P. *J. Chem. Phys.* **1997**, *106*, 9382–9385.
(22) Nie, S.; Feibelman, P. J.; Bartelt, N. C.; Thürmer, K. *Phys. Rev. Lett.* **2010**, *105*, 026102.

(23) Jacobi, K.; Bedürftig, K.; Wang, Y.; Ertl, G. *Surf. Sci.* **2001**, *472*, 9–20.
(24) Daschbach, J. L.; Peden, B. M.; Smith, R. S.; Kay, B. D. *J. Chem. Phys.* **2004**, *120*, 1516–1523.
(25) Fisher, G. B.; Gland, J. L. *Surf. Sci.* **1980**, *94*, 446–455.
(26) Su, X.; Lianos, L.; Shen, Y. R.; Somorjai, G. A. *Phys. Rev. Lett.* **1998**, *80*, 1533–1536.
(27) van der Niet, M. J. T. C.; Dominicus, I.; Koper, M. T. M.; Juurlink, L. B. F. *Phys. Chem. Chem. Phys.* **2008**, *10*, 7169–7179.
(28) van der Niet, M. J. T. C.; den Dunnen, A.; Juurlink, L. B. F.; Koper, M. T. M. *J. Chem. Phys.* **2010**, *132*, 174705.
(29) Picolin, A.; Busse, C.; Redinger, A.; Morgenstern, M.; Michely, T. *J. Phys. Chem. C* **2009**, *113*, 691–697.
(30) Luntz, A. C.; Grimblot, J.; Fowler, D. E. *Phys. Rev. B* **1989**, *39*, 12903–12906.
(31) Gland, J. L.; Sexton, B. A.; Fisher, G. B. *Surf. Sci.* **1980**, *95*, 587–602.
(32) Campbell, C. T.; Ertl, G.; Kuipers, H.; Segner, J. *Surf. Sci.* **1981**, *107*, 220–236.
(33) Gee, A. T.; Hayden, B. E. *J. Chem. Phys.* **2000**, *113*, 10333–10343.
(34) Schwaha, K.; Bechtold, E. *Surf. Sci.* **1977**, *65*, 277–286.
(35) Parker, D. H.; Bartram, M. E.; Koel, B. E. *Surf. Sci.* **1989**, *217*, 489–510.
(36) Starke, U.; Heinz, K.; Materer, N.; Wander, A.; Michl, M.; Döll, R.; van Hove, M. A.; Somorjai, G. A. *J. Vac. Sci. Technol. A* **1992**, *10*, 2521–2528.
(37) Starke, U.; Materer, N.; Barbieri, A.; Döll, R.; Heinz, K.; van Hove, M. A.; Somorjai, G. A. *Surf. Sci.* **1993**, *287/288*, 432–437.
(38) Materer, N.; Starke, U.; Barbieri, A.; Döll, R.; Heinz, K.; Van Hove, M. A.; Somorjai, G. A. *Surf. Sci.* **1995**, *325*, 207–222.
(39) Feibelman, P. J.; Esch, S.; Michely, T. *Phys. Rev. Lett.* **1996**, *77*, 2257–2260.
(40) Mortensen, K.; Klink, C.; Jensen, F.; Besenbacher, F.; Stensgaard, I. *Surf. Sci.* **1989**, *220*, L701–L708.
(41) Getman, R. B.; Xu, Y.; Schneider, W. F. *J. Phys. Chem. C* **2008**, *112*, 9559–9572.
(42) Gland, J. L.; Korchak, V. N. *Surf. Sci.* **1978**, *75*, 733–750.
(43) Gland, J. L. *Surf. Sci.* **1980**, *93*, 487–514.
(44) Fiorin, V.; Borthwick, D.; King, D. A. *Surf. Sci.* **2009**, *603*, 1360–1364.
(45) Rar, A.; Matsushima, T. *Surf. Sci.* **1994**, *318*, 89–96.
(46) Wang, H.; Tobin, R. G.; Lambert, D. K.; DiMaggio, C. L.; Fisher, G. B. *Surf. Sci.* **1997**, *372*, 267–278.
(47) Gambardella, P.; Šljivančanin, Ž.; Hammer, B.; Blanc, M.; Kuhnke, K.; Kern, K. *Phys. Rev. Lett.* **2001**, *87*, 056103.
(48) Šljivančanin, Ž.; Hammer, B. *Surf. Sci.* **2002**, *515*, 235–244.
(49) Yamanaka, T.; Matsushima, T.; Tanaka, S.-I.; Kamada, M. *Surf. Sci.* **1996**, *349*, 119–128.
(50) Heyd, D. V.; Scharff, R. J.; Yates, J. T., Jr. *J. Chem. Phys.* **1999**, *110*, 6939–6946.
(51) Winkler, A.; Guo, X.; Siddiqui, H. R.; Hagans, P. L.; Yates, J. T., Jr. *Surf. Sci.* **1988**, *201*, 419–443.
(52) Siddiqui, H. R.; Winkler, A.; Guo, X.; Hagans, P.; Yates, J. T., Jr. *Surf. Sci.* **1988**, *193*, L17–L23.
(53) Sano, M.; Seimiya, Y.; Ohno, Y.; Matsushima, T.; Tanaka, S.-I.; Kamada, M. *Surf. Sci.* **1999**, *421*, 386–396.
(54) Fisher, G. B.; Sexton, B. A. *Phys. Rev. Lett.* **1980**, *44*, 683–686.
(55) Schiros, T.; Näslund, L. Å.; Andersson, K.; Gyllenpalm, J.; Karlberg, G. S.; Odelius, M.; Ogasawara, H.; Pettersson, L. G. M.; Nilsson, A. *J. Phys. Chem. C* **2007**, *111*, 15003–15012.
(56) Creighton, J. R.; White, J. M. *Surf. Sci.* **1982**, *122*, L648–L652.
(57) Bedürftig, K.; Völkening, S.; Wang, Y.; Wintterlin, J.; Jacobi, K.; Ertl, G. *J. Chem. Phys.* **1999**, *111*, 11147–11154.
(58) Michaelides, A.; Hu, P. *J. Am. Chem. Soc.* **2001**, *123*, 4235–4242.
(59) Michaelides, A.; Hu, P. *J. Chem. Phys.* **2001**, *114*, 513–519.
(60) Clay, C.; Haq, S.; Hodgson, A. *Phys. Rev. Lett.* **2004**, *92*, 046102.
(61) Karlberg, G. S. *Phys. Rev. B* **2006**, *74*, 153414.
(62) Held, G.; Clay, C.; Barrett, S. D.; Haq, S.; Hodgson, A. *J. Chem. Phys.* **2005**, *123*, 064711.
(63) Li, X.-Z.; Probert, M. I. J.; Alavi, A.; Michaelides, A. *Phys. Rev. Lett.* **2010**, *104*, 066102.
(64) Zimbitas, G.; Gallagher, M. E.; Darling, G. R.; Hodgson, A. *J. Chem. Phys.* **2008**, *128*, 074701.
(65) Karlberg, G. S.; Wahnström, G.; Clay, C.; Zimbitas, G.; Hodgson, A. *J. Chem. Phys.* **2006**, *124*, 204712.
(66) Berná, A.; Climent, V.; Feliu, J. M. *Electrochem. Commun.* **2007**, *9*, 2789–2794.
(67) Lebedeva, N. P.; Rodes, A.; Feliu, J. M.; Koper, M. T. M.; van Santen, R. A. *J. Phys. Chem. B* **2002**, *106*, 12938–12947.
(68) van der Niet, M. J. T. C.; den Dunnen, A.; Juurlink, L. B. F.; Koper, M. T. M. *Angew. Chem., Int. Ed.* **2010**, *49*, 6572–6575.
(69) Jenniskens, H. G.; Bot, A.; Dorlandt, P. W. F.; van Essenberg, W.; van Haas, E.; Kleyn, A. W. *Meas. Sci. Technol.* **1997**, *8*, 1313–1322.
(70) Riedmüller, B.; Giskes, F.; Glastra van Loon, D.; Lassing, P.; Kleyn, A. W. *Meas. Sci. Technol.* **2002**, *13*, 141–149.
(71) van Hove, M. A.; Somorjai, G. A. *Surf. Sci.* **1980**, *92*, 489–518.
(72) Sachs, C.; Hildebrand, M.; Völkening, S.; Wintterlin, J.; Ertl, G. *Science* **2001**, *293*, 1635–1638.
(73) Sachs, C.; Hildebrand, M.; Völkening, S.; Wintterlin, J.; Ertl, G. *J. Chem. Phys.* **2002**, *116*, 5759–5773.
(74) Petrik, N. G.; Kimmel, G. A. *J. Chem. Phys.* **2004**, *121*, 3727–3735.
(75) van der Niet, M. J. T. C.; den Dunnen, A.; Juurlink, L. B. F.; Koper, M. T. M. *Phys. Chem. Chem. Phys.* Accepted.

JP106412E